Limitations of IL-2 and Rapamycin in Immunotherapy of Type 1 Diabetes

Audrey Baeyens,[1,2,3] Louis Pérol,[1,2,3] Gwladys Fourcade,[1,2,3] Nicolas Cagnard,[4,5] Wassila Carpentier,[1,6] Janine Woytschak,[7] Onur Boyman,[7,8] Agnès Hartemann,[9,10] and Eliane Piaggio[1,2,3]

Administration of low-dose interleukin-2 (IL-2) alone or combined with rapamycin (RAPA) prevents hyperglycemia in NOD mice. Also, low-dose IL-2 cures recent-onset type 1 diabetes (T1D) in NOD mice, partially by boosting pancreatic regulatory T cells (T_{reg} cells). These approaches are currently being evaluated in humans. Our objective was to study the effect of higher IL-2 doses (250,000–500,000 IU daily) as well as low-dose IL-2 (25,000 IU daily) and RAPA (1 mg/kg daily) (RAPA/IL-2) combination. We show that, despite further boosting of T_{reg} cells, high doses of IL-2 rapidly precipitated T1D in prediabetic female and male mice and increased myeloid cells in the pancreas. Also, we observed that RAPA counteracted IL-2 effects on T_{reg} cells, failed to control IL-2–boosted NK cells, and broke IL-2–induced tolerance in a reversible way. Notably, the RAPA/IL-2 combination failure to cure T1D was associated with an unexpected deleterious effect on glucose homeostasis at multiple levels, including β-cell division, glucose tolerance, and liver glucose metabolism. Our data help to understand the therapeutic limitations of IL-2 alone or RAPA/IL-2 combination and could lead to the design of improved therapies for T1D. ***Diabetes*** **62:3120–3131, 2013**

In type 1 diabetes (T1D), the immune system destroys the pancreatic β-cells (1). At clinical onset, ~30% of β-cells are still able to produce insulin (2), thus stopping autoimmune destruction, which at this stage is a promising approach (3). Along the same lines, there is a growing list of phase I/II clinical trials based on immunomodulation that are currently being conducted in T1D patients (4).

NOD mice, which develop spontaneous T1D, represent an accepted model for testing new therapies (5), the gold standard being that treatments that cure overt hyperglycemia in these mice may be most appropriate for translation into the clinic, as was the case for anti-CD3 antibodies (Abs) (6), which have been tested in patients with promising results (7). In addition, results from our own group showing that low-dose interleukin-2 (IL-2) can prevent (8) and revert disease in NOD mice (9) have led to the translation of this strategy into clinical trials in T1D patients (clinical trial reg. no. NCT01353833, clinicaltrials.gov).

We have shown that in NOD mice, administration of low-dose IL-2 for 5 days induced the remission of new-onset T1D by specifically boosting regulatory T cells (T_{reg} cells) in the pancreas without activating pathogenic effector T cells (T_{eff} cells). However, remission was obtained in only 60% of treated mice, and half of them became diabetic again during the following months (9). Consequently, improving IL-2 therapy by optimizing dosing or combining IL-2 with other immunomodulatory drugs, such as rapamycin (RAPA), could be of great importance for the goal of translating this therapy to humans.

RAPA has been used in clinical transplantation for many years (10), and it has been safely administered to T1D patients during islet transplantation (11,12). In mice, RAPA monotherapy can prevent T1D development (13); however, it is unable to induce disease reversal (14). Moreover, RAPA and IL-2 were found to be synergistic for the prevention of diabetes in NOD mice (13). Consequently, we decided to test whether RAPA could synergize with short-term IL-2 therapy to reverse T1D and reinforce the development of long-term tolerance.

In this work, we have further studied the mechanisms of action of IL-2 and RAPA alone or in combination in the NOD model of T1D.

RESEARCH DESIGN AND METHODS

Mice. NOD mice were bred in our animal facility under specific pathogen-free conditions in agreement with current European legislation. Protocols were approved by The Ethics Committee in Animal Experiment Charles Darwin, France (no. Ce5/2012/021).

IL-2 and RAPA treatment. Mice were treated with daily intraperitoneal injections of 25,000, 250,000, or 500,000 IU of recombinant human IL-2 (Proleukin; Novartis France) for the indicated time. RAPA (Rapamune; Wyeth-Lederle) was administered at 1 mg/kg per os, a dose that has been previously reported not to be toxic to pancreatic islets (13,14) and to prevent T1D onset in NOD mice (13). Glycosuria was measured using colorimetric strips (Multistix; Bayer), and blood glucose levels were quantified by a glucometer (Optium Xceed; Abbott).

Spleen-, lymph node–, and tissue-infiltrating lymphocytes preparation. Spleen and lymph nodes (LNs; axillary and brachial) and pancreatic draining LNs (DLNs) were isolated and dissociated in PBS-3% FCS. For pancreas-infiltrating lymphocyte preparation, the whole pancreas was digested with collagenase/DNase solution and submitted to Percoll density gradient as described (15,16).

Abs and flow cytometry analysis. Anti-CD3, anti-CD4, anti-CD8, anti-CD45.1, anti-inducible T-cell costimulator (ICOS), anti-B220, anti-glucocorticoid–induced tumor necrosis factor receptor (GITR), anti-Ly6C, anti-Ly6G, anti-CD11b, anti-CD11c, anti-CD19, anti-Gr1, anti–IFN-γ, anti-Ki67, anti-pSTAT5 (pY694), and streptavidin labeled with phycoerythrin (PE), allophycocyanin, PerCP, PercP-Cy5.5, V500, allophycocyanin (APC)-H7, PE-Cy7, Alexa Fluor-700, Alexa Fluor-647, or biotin, were from BD Biosciences. Anti-CD25, anti-cytotoxic

From [1]Université Pierre et Marie Curie, Paris, France; [2]Centre National de la Recherche Scientifique, UMR 7211, Paris, France; the [3]Department of Immunology-Immunopathology-Immunotherapy, INSERM U959, Paris, France; [4]INSERM U580, Paris, France; the [5]Bioinformatics Platform, Faculty of Medicine Paris Descartes, Hôpital Necker-Enfants Malades, Paris, France; [6]Plate-forme Post-Génomique P3S, Université Pierre et Marie Curie, Faculty of Medicine, Paris, France; the [7]Laboratory of Applied Immunobiology, University of Zurich, Zurich, Switzerland; the [8]Allergy Unit, Department of Dermatology, University Hospital Zurich, Zurich, Switzerland; the [9]Department of Endocrinology, Nutrition and Diabetes, Assistance Publique-Hôpitaux de Paris, Pitié-Salpêtrière-Charles Foix Hospital, Paris, France; and the [10]Department of Medicine Faculty, Université Pierre et Marie Curie, Paris, France.
Corresponding author: Eliane Piaggio, elianepiaggio@yahoo.com.
Received 8 February 2013 and accepted 8 May 2013.
DOI: 10.2337/db13-0214
This article contains Supplementary Data online at http://diabetes.diabetesjournals.org/lookup/suppl/doi:10.2337/db13-0214/-/DC1.
A.B. and L.P. contributed equally to this study.
E.P. and L.P. are currently affiliated with INSERM 932, Paris, France, and Centre de Recherche, Laboratoire d'Immunologie Clinique, Institut Curie, Paris, France.

T-lymphocyte antigen 4 (CTLA-4), anti-NKp46, and anti-F4/80 labeled with fluorescein isothiocyanate (FITC), PE-Cy7, APC, or eFluor 450 were from eBiosciences. The eFluor 450-anti-Foxp3 staining was performed using the eBioscience kit. For intracellular cytokine staining, cells were restimulated with 1 μg/mL phorbol myristic acid (PMA)/0.5 μg/mL Ionomycin (Sigma) for 3 h in the presence of GolgiPlug (1 μL/mL) (BD Biosciences). For phospho-STAT-5 staining, DLNs were dissociated, immediately fixed in PBS 1.5% formaldehyde, and permeabilized in MeOH. Cells were stained in PBS 0.2% BSA medium containing anti-CD4, anti-CD25, anti-Foxp3, and anti-pSTAT5 monoclonal Abs. PE-conjugated NRP-V7/H-2^K tetramer containing NRP-V7 peptide (KYNKANVFL) and control PE-conjugated TUM/H-2^K tetramer containing TUM peptide (KYQAVTTTL) were provided by Pere Santamaria. Cells were stained in RPMI 2% medium containing NRP-V7/H-2K or TUM/H-2K at room temperature for 2 h, washed, and further stained with anti-CD8 and anti-CD4 Abs. Cells were acquired on a LSR II (BD Biosciences) and analyzed with FlowJo (Tree Star) software.

Histology. Pancreata were fixed in 10% formalin, embedded in paraffin, cut into 2-μm-thick sections, and stained with hematoxylin/eosin. Insulitis scoring was evaluated microscopically.

For immunohistology, pancreata were embedded in optimal cutting temperature medium, snap-frozen in liquid nitrogen, and stored at −80°C until use. The 8-μm-thick sections were blocked with PBS 2% BSA and stained with anti-mouse insulin (Sigma) followed by biotinylated anti-mouse IgG1 (Abcam) and APC-labeled streptavidin, PE-labeled anti-CD45.1, and FITC-labeled anti-Ki67 (BD Biosciences) and counterstained with Hoechst (Dako). Proliferating β-cells were defined as $Ki67^+$ $insulin^+$ $CD45.1^-$ and manually counted. For CD11b staining, FITC anti-CD11b (BD Biosciences) was used. Images were acquired on a Leica epifluorescence microscope and analyzed with Metavue Software.

Determination of wet weight of organs. Organs were weighed before and after lyophilization overnight at 58°C under vacuum, and wet weight was calculated by subtracting the initial weight from the weight after lyophilization, as described (17).

Glucose/insulin tolerance test. Twelve-week-old nondiabetic NOD female mice were treated for 5 days with PBS, 25,000 IU IL-2, IL-2, RAPA, or 25,000 IU IL-2 plus RAPA, and the last administration was performed 2 h before the beginning of the intraperitoneal glucose tolerance test (IPGTT)/insulin tolerance test (ITT). For IPGTTs, a single dose of 2 g glucose/kg was injected intraperitoneally after 16 h overnight fast. For ITTs, a single dose of 0.75 IU insulin/kg (Humulin R; Lilly) was injected intraperitoneally after 4 h fasting, and blood glucose levels were determined.

Sample generation and DNA microarray hybridization and analysis. Twelve-week-old nondiabetic NOD female mice were treated for 5 days with PBS, 25,000 IU IL-2, RAPA, or IL-2 plus RAPA. Mice were fasted for 16 h before the injection of a glucose bolus (2 g/kg) 2 h after the last administration of IL-2 and/or RAPA. Four hours after the glucose challenge, mice were killed, perfused with 0.9% NaCl, and liver was collected. Tissue was processed (TissueLyser II; Qiagen), and RNA was generated (RNeasy Mini kit; Qiagen). RNA quality was verified in an Agilent Bioanalyzer and measured with a Nanodrop 1000 (Thermo Scientific).

Microarray experiments were performed on Illumina MouseWG-6 BeadChip. Data were quantile normalized using BeadStudio software. The working lists were created by filtering probes with detection P values <0.05 for all the chips and discarding overlapping probes. Each dataset was derived from three biologically independent replicate samples. Independent samples were compared by computing fold ratios and were filtered at a 1.5-fold threshold for Venn Diagrams and a 1.2-fold threshold for pathway analysis. For pathway analysis, GenBank accession numbers were mapped to the Ingenuity database (IPA, http://www.ingenuity.com) to retrieve relevant biological processes (microarray data accession number: E-MEXP-3789).

Statistical analyses. Statistical significance was calculated using a two-tailed unpaired Student t test with 95% CIs. When sample distribution was not normal (as determined by a D'Agostino and Pearson omnibus normality test), a Mann-Whitney-Wilcoxon nonparametric test was used. Survival proportions were calculated using the Kaplan-Meier method, and statistical significance was calculated using the Gehan-Breslow-Wilcoxon test. All statistical significances were calculated with GraphPad Prism v5.0 software.

RESULTS

High doses of IL-2 are toxic and can precipitate T1D development. We have previously shown that five doses of 25,000 IU IL-2 could revert new-onset T1D in NOD mice in part by specifically boosting pancreatic T_{reg} cells (9). However, not all treated mice were cured, and in some of them the beneficial effects were transient. We reasoned that increasing the dose of IL-2 administered may further increase the frequency of T_{reg} cells and thus improve the treatment efficacy.

We first tested the capacity of higher IL-2 doses to prevent T1D development. We found that daily treatment of NOD mice with 250,000 or 500,000 IU IL-2 (i.e., doses 10- or 20-fold higher than the dose shown to prevent T1D) (8) could be lethally toxic in a dose-dependent manner in 5-week-old mice (Fig. 1*A*, *top*). In prediabetic mice at 12–14 weeks of age, this treatment was less toxic, but it dramatically precipitated the onset of diabetes after only a few daily injections and in a dose-dependent manner (Fig. 1*A*, *middle* and *bottom*). At the 250,000 IU IL-2 dose, females were significantly more sensitive than males to IL-2–induced acceleration of diabetes (Fig. 1*A*, *bottom*).

IL-2 toxicity is mainly associated with vascular leak syndrome, which can lead to hypotension, pulmonary edema, liver cell damage, and even death (17). We thus measured organ edema after 5 days of high-dose IL-2 administration (Fig. 1*B*). Unlike C57BL/6 mice (17), higher cumulative doses of IL-2 were necessary before vascular leak syndrome became evident in NOD mice. Moreover, we observed sex-dependent differences, with lung edema being most prominent in males and liver edema in females. Brain edema did not develop in either group. Additionally, we measured islet infiltration in these mice and observed that 5 days of high-dose IL-2 administration induced a mild increase of invasive insulitis in males (Fig. 1*C*).

The rapid onset of T1D, observed as early as after only 3 days of treatment, was not due to an immediate detrimental effect of IL-2 on glucose homeostasis, as administration of 250,000 IU IL-2 did not induce any apparent alteration in glucose metabolism after a glucose bolus administration 2 h after the IL-2 injection (Fig. 1*D*).

Low-dose IL-2–induced T1D remission was associated with T_{reg}-cell activation only in the pancreas, whereas T_{eff}, $CD8^+$, and NK cells were not noticeably affected by this treatment (9). On the contrary, high-dose IL-2 induced systemic effects, including increased cell numbers in secondary lymphoid organs, most significantly in the pancreas DLN (Fig. 2*A*). In the DLN (Fig. 2*B*), nondraining LNs, and spleen (not shown), significantly higher proportions of NK cells along with lower frequencies of total $CD4^+$ T cells, but with increased T_{reg}-cell proportions, were observed.

In the islets, high-dose IL-2 effects were more pronounced (Fig. 2*B*). Notably, total $CD4^+$ T cells were unchanged, but an almost double frequency of T_{reg} cells was seen after IL-2 treatment. Also, NK, $CD11c^+$, and $CD11b^+$ cells increased after IL-2 administration. Interestingly, in almost all analyzed organs, T_{reg}, T_{eff}, $CD8^+$, NK, B, and $CD11b^+$ cells increased their division after high-dose IL-2 administration, as assessed by quantification of Ki67 expression (Fig. 2*C*). In particular, >80% of NK and $CD11b^+$ cells had cycled in the pancreas. Indeed, by immunohistology analysis these highly proliferative $CD11b^+$ cells were found interspersed around the islets and surrounding blood vessels (Fig. 3*A*). Further phenotypic analysis indicated that two subpopulations among $CD11b^+$ cells increased during IL-2 treatment: $CD11b^+$ $Ly6C^+$ $F4/80^+$ cells, likely representing tissue macrophages; and $CD11b^+$ $Ly6G^+$ cells, likely representing neutrophils (18) (Fig. 3*B*).

Detailed analysis of the effects of IL-2 on T_{reg} cells indicated that the cytokine increased the expression of Foxp3 and CD25 in a dose-dependent way, suggesting an enhancement of T_{reg} cell fitness (Fig. 4*A*). Similarly, even though the frequency of T_{eff} cells was diminished, their activation was potentiated by IL-2 administration, as

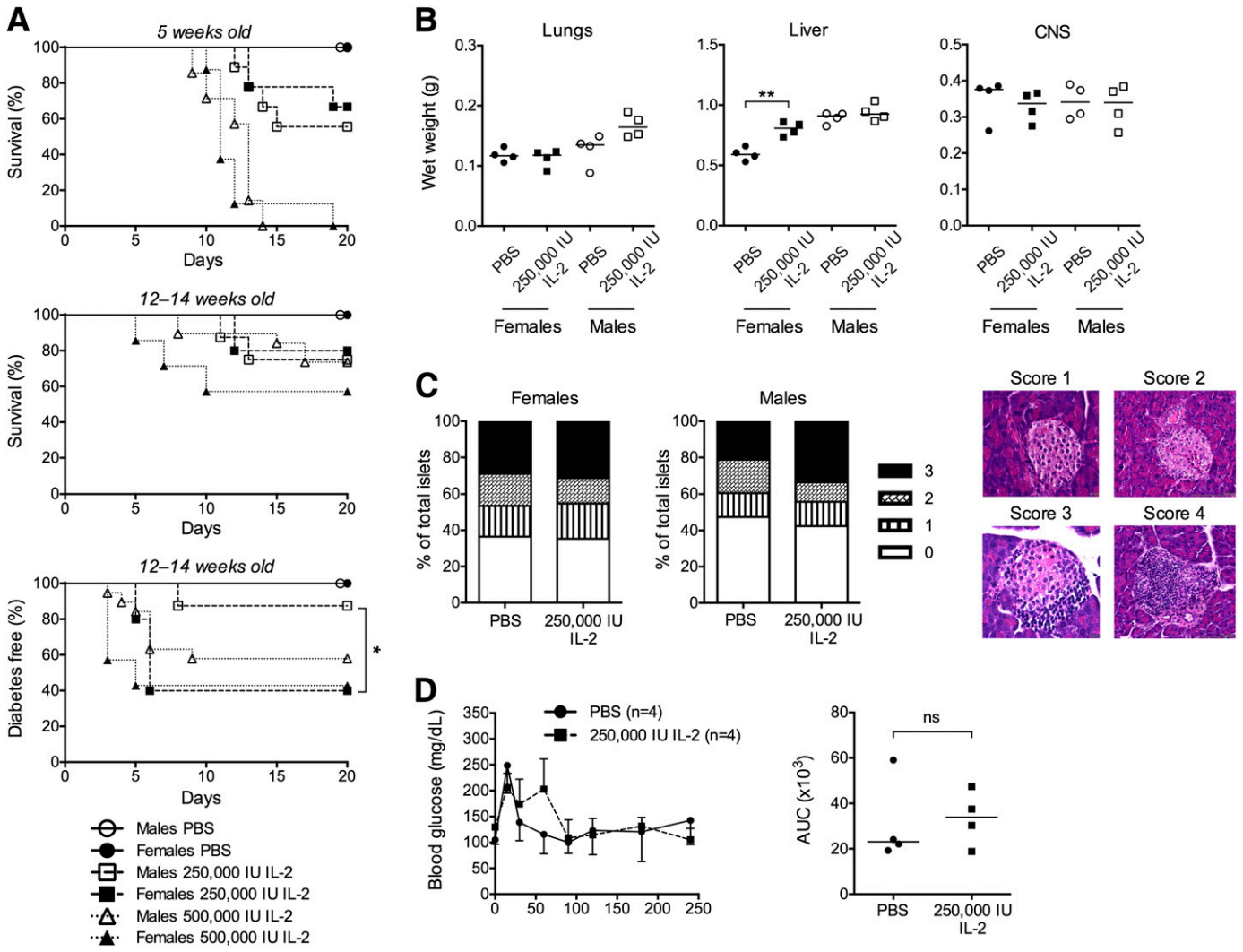

FIG. 1. Administration of high doses of IL-2 to NOD mice: toxicity and diabetes development. *A*: Male and female NOD mice 5 weeks of age (*top*) or 12–14 weeks of age (*middle* and *bottom*) were injected daily with PBS (●, females; ○, males), 250,000 IU IL-2 (■, females; □, males), or 500,000 IU IL-2 (▲, females; △, males) over 20 days. Shown are Kaplan-Meier survival curves of treated mice (*top* and *middle*) and the percentage of diabetes-free mice; *$P < 0.05$ (Gehan-Breslow-Wilcoxon test) (*bottom*). *B* and *C*: Male and female NOD mice 12–14 weeks of age were injected for 5 days with PBS (●, females; ○, males,) or 250,000 IU IL-2 (■, females; □, males) and analyzed 2 h after the last injection. *B*: Wet weight of lungs (*left*), liver (*middle*), and CNS (*right*) was determined. Symbols represent individual mice and horizontal lines represent the median. **$P < 0.01$ (unpaired, two-tailed Student *t* test). *C*: Histological quantification of islet infiltration by immune cells in female and male NOD mice. Shown are the percentages of islets with no infiltration (0), peri-insulitis (1), moderate insulitis with <50% islet area infiltrated by immune cells (2), and severe insulitis with more than 50% islet area infiltrated by immune cells (3). Pictures show representative islets corresponding to the insulitis score used for analysis. *D*: Prediabetic female NOD mice 12–16 weeks of age were fasted for 4 h and injected with PBS or 250,000 IU IL-2 followed by a glucose bolus 2 h later. Results are presented as blood glucose levels during the 4-h follow-up (*left*) and as area under the blood–glucose curve (AUC) during the follow-up period (*right*), symbols represent individual mice, and horizontal lines represent the median. Data are cumulative of two (*A*, *top*) to five (*A*, *middle* and *bottom*) independent experiments or are representative of one (*B* and *C*) to three (*D*) independent experiments. ns, not significant.

indicated by the dose-dependent increase in the fraction of $CD25^+$ T_{eff} and $CD8^+$ T cells, mainly observed in the islets (Fig. 4*B*). Moreover, T_{eff}, $CD8^+$, and NK cells showed increased IFN-γ production (Fig. 4*C*) during treatment with high-dose IL-2. Additionally, among the expanded $CD8^+$ T-cell population, we observed a significant increase in the frequencies of $NRPV7^+$ islet-specific glucose-6-phosphatase catalytic subunit-related protein-specific autoreactive CD8 T cells (19) in the blood and the islets of the treated mice (Fig. 4*D*).

RAPA partially counteracts the activation of pancreatic T_{reg} cells induced by low-dose IL-2. The immunomodulatory effects of RAPA have been attributed to its capacity to preferentially affect activated T_{eff} cells, while T_{reg} cells are less susceptible to its action (20). Consequently, we hypothesized that the beneficial effect of low-dose IL-2 on T_{reg} cells could synergize with the concomitant elimination of pathogenic T_{eff} cells by RAPA after administration of a RAPA/low-dose IL-2 combination.

We analyzed the effects of combined treatment on lymphoid cells in prediabetic NOD females, in which insulitis is already important. Administration for 5 days of RAPA alone, low-dose IL-2 alone, or both drugs combined did not induce major changes in absolute numbers and frequencies of T cells in the spleen, LNs, and DLN (data not shown). In the pancreas, low-dose IL-2 alone did not modify the frequency of total $CD8^+$ or $CD4^+$ T cells (data not shown). However, it modified the T_{reg}/T_{eff} balance by increasing the

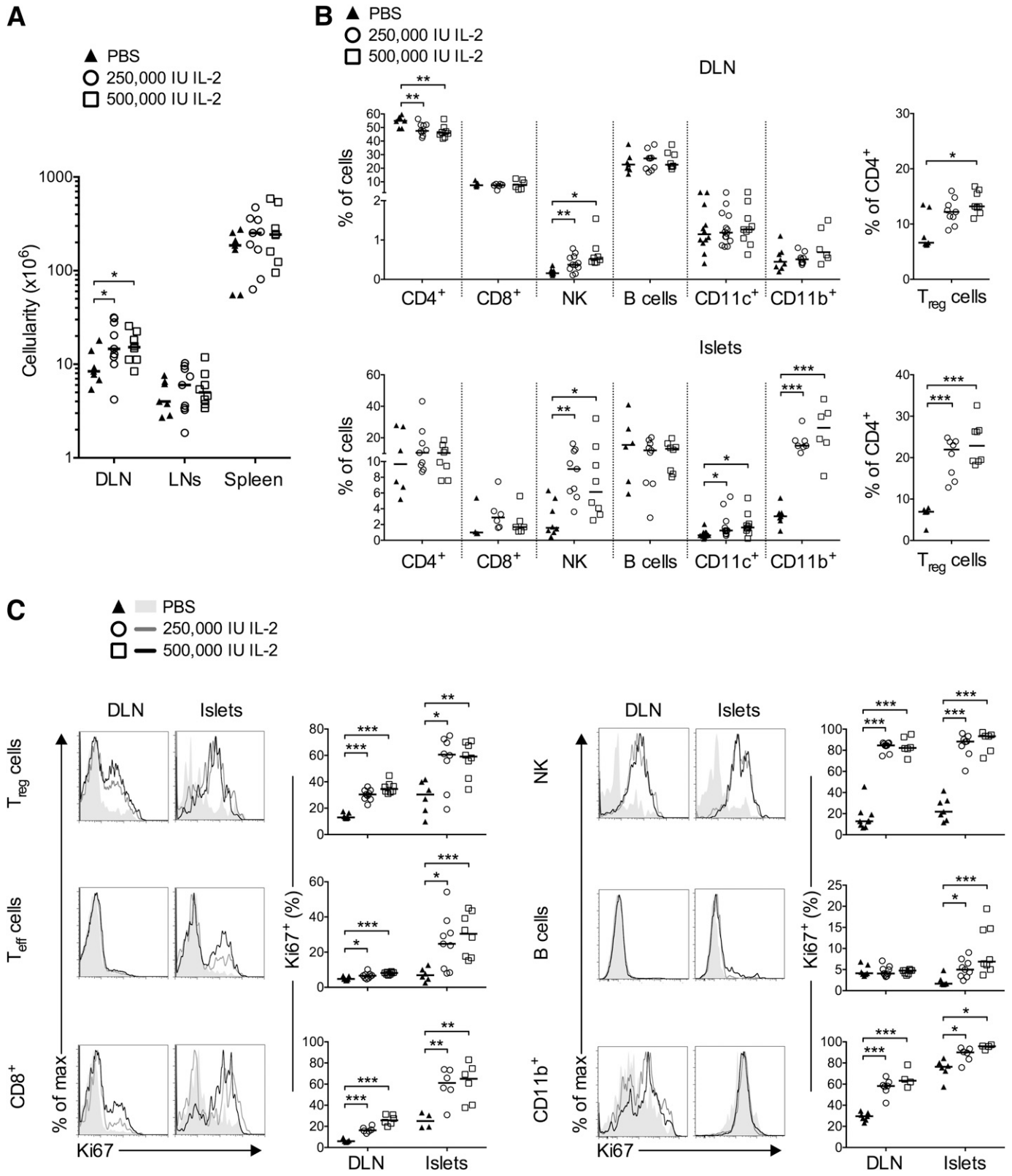

FIG. 2. Administration of high doses of IL-2 to NOD mice: effects on immune cells. Prediabetic female NOD mice 12–14 weeks of age were treated daily with PBS or 250,000 or 500,000 IU IL-2 over 5 days and analyzed 2 h after the last injection. *A*: Absolute cell numbers in DLN, nondraining LNs, and spleen. *B*: Percentage of total $CD4^+$, $CD8^+$, $NKp46^+$ $CD3^-$ (NK), B, $CD11c^+$, and myeloid $CD11b^+$ cells in DLN (*top*) or in pancreas (*bottom*). *Right panels* indicate the percentage of T_{reg} cells among total $CD4^+$ T cells. *C*: Representative histograms of Ki67 expression (*left*) and percentages of $Ki67^+$ cells among indicated populations (*right*) in the DLN and pancreas. Similar results were obtained in male NOD mice (data not shown). Data are cumulative of three to five independent experiments with 4 to 14 mice per group. Symbols represent individual mice, and horizontal lines represent the median. *$P < 0.05$; **$P < 0.01$; ***$P < 0.001$ (unpaired, two-tailed Student *t* test).

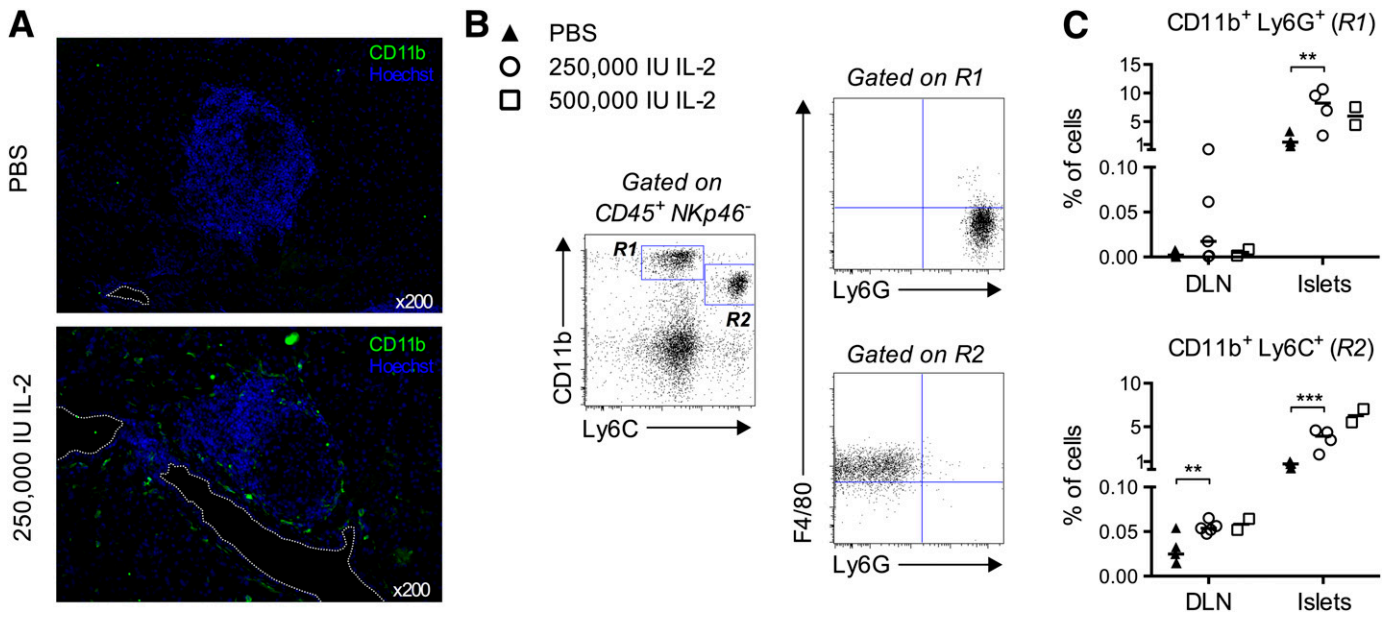

FIG. 3. Administration of high doses of IL-2 to NOD mice: effects on myeloid cells. Mice were treated as in Figure 2. *A*: Representative immunofluorescence of cryosections from the pancreas of mice treated with PBS (*top*) or 250,000 IU IL-2 (*bottom*), stained with anti-CD11b Abs (green) and Hoechst (blue) (magnification ×200). Dashed line indicates blood vessels. *B*: Myeloid cell-gating strategy: islet-infiltrating cells were pregated as CD45$^+$ NKp46$^-$, and expression of CD11b versus Ly6C was used to define gates R1 and R2 as shown. Cells in these gates were further analyzed for the expression of F4/80 and Ly6G. Cells in gate R1 were mostly F4/80$^-$ and Ly6G$^+$, probably representing neutrophils, and cells in gate R2 were mostly F4/80$^+$ and Ly6G$^-$, probably representing tissue macrophages. *C*: Percentages of cells in gate R1 (*top*) and R2 (*bottom*) in islets, DLN, LNs, and spleen of mice in indicated treatment groups. Data are cumulative of two independent experiments with two to five mice per condition, except for *A*, which is from one experiment with three mice per group. Symbols represent individual mice and horizontal lines represent the median. **$P < 0.01$; ***$P < 0.001$ (unpaired, two-tailed Student *t* test).

percentage of T_{reg} cells (Fig. 5*A*), which was associated with increased cell division (Fig. 5*B*) and increased expression of Foxp3, CD25, GITR, ICOS, and CTLA-4 (Fig. 5*C*). A similar tendency was observed when low-dose IL-2 was combined with RAPA. Notably, the effect of IL-2 on T_{reg} cell numbers or activation was significantly less pronounced in the presence of RAPA (Fig. 5*A–C*).

Finally, we examined the effects of treatment on NK cells in the pancreas and observed that their proportion doubled after 5 days of treatment with low-dose IL-2 alone, with the percentage of proliferating cells increasing from low basal levels up to ~60% after treatment (Fig. 5*D–E*). Addition of RAPA to IL-2 treatment did not modify the effect of IL-2 on NK cells.

We discarded that the partial counteraction of IL-2 effects on T_{reg} cells by RAPA was due to interference of the JAK/STAT pathway, as IL-2–mediated STAT5 phosphorylation was not modified by the administration of RAPA in vivo (Fig. 6).

RAPA inhibits the ability of low-dose IL-2 to revert T1D. To test whether RAPA could reinforce the development of long-term tolerance when combined with IL-2, we treated new-onset T1D NOD mice with 25,000 IU (low-dose) IL-2 with or without RAPA. In agreement with our previously reported results (9), low-dose IL-2 treatment induced diabetes remission in 57% of the mice. However, none of the 12 mice that received the combined treatment were cured (Fig. 7*A*). We assessed the effects of treatment on pancreatic T cells from these mice: RAPA/IL-2 combination did not modify the percentage of total CD8$^+$ or CD4$^+$ T cells (not shown), but it significantly increased the frequency of T_{reg} cells (Fig. 7*B*). Interestingly, RAPA hampered the IL-2–induced reduction in IFN-γ production by CD8$^+$ T cells infiltrating the pancreas (Fig. 7*C*), which we had previously shown to be associated with T1D reversal (9). These results may partially explain why RAPA inhibits the ability of IL-2 to revert disease.

To determine whether RAPA had any effect in mice that had reverted from new-onset T1D after low-dose IL-2 therapy, we administered RAPA to NOD mice 10 days after IL-2–induced disease remission. Surprisingly, RAPA precipitated hyperglycemia in all previously cured mice (Fig. 7*D*). Of note, in two of eight treated mice, RAPA induced irreversible hyperglycemia, but in the other six IL-2–treated mice, the hyperglycemia triggered by RAPA was transient. Indeed, after RAPA withdrawal and without further addition of IL-2, mice spontaneously became normoglycemic again until RAPA treatment was resumed, at which point mice reversed to diabetes. In some of these mice, the transient occurrence of diabetes upon adding and removing RAPA could be repeated at least three times, indicating that RAPA can reversibly inhibit the tolerogenic effect of IL-2. We analyzed the temporal effect of RAPA on the pancreatic infiltrate. Intriguingly, T_{reg}-cell levels in the pancreas were significantly lower in mice cured of diabetes with IL-2, but which had become diabetic again after RAPA treatment, compared with mice that did not receive RAPA, and a significant parallel increase in these cells was observed in the DLN (Fig. 7*E* and *F*). T_{reg} cells returned to initial levels after RAPA withdrawal and restoration of euglycemia, suggesting that under RAPA treatment the migration pattern of CD4$^+$ T cells may be altered.

Combination IL-2 plus RAPA impairs glucose tolerance. The rapid reversibility of the effect of RAPA on diabetes led us to evaluate whether RAPA was affecting glucose homeostasis. We measured fasting blood glucose levels and performed glucose tolerance tests in prediabetic NOD mice previously treated with IL-2, RAPA, or both

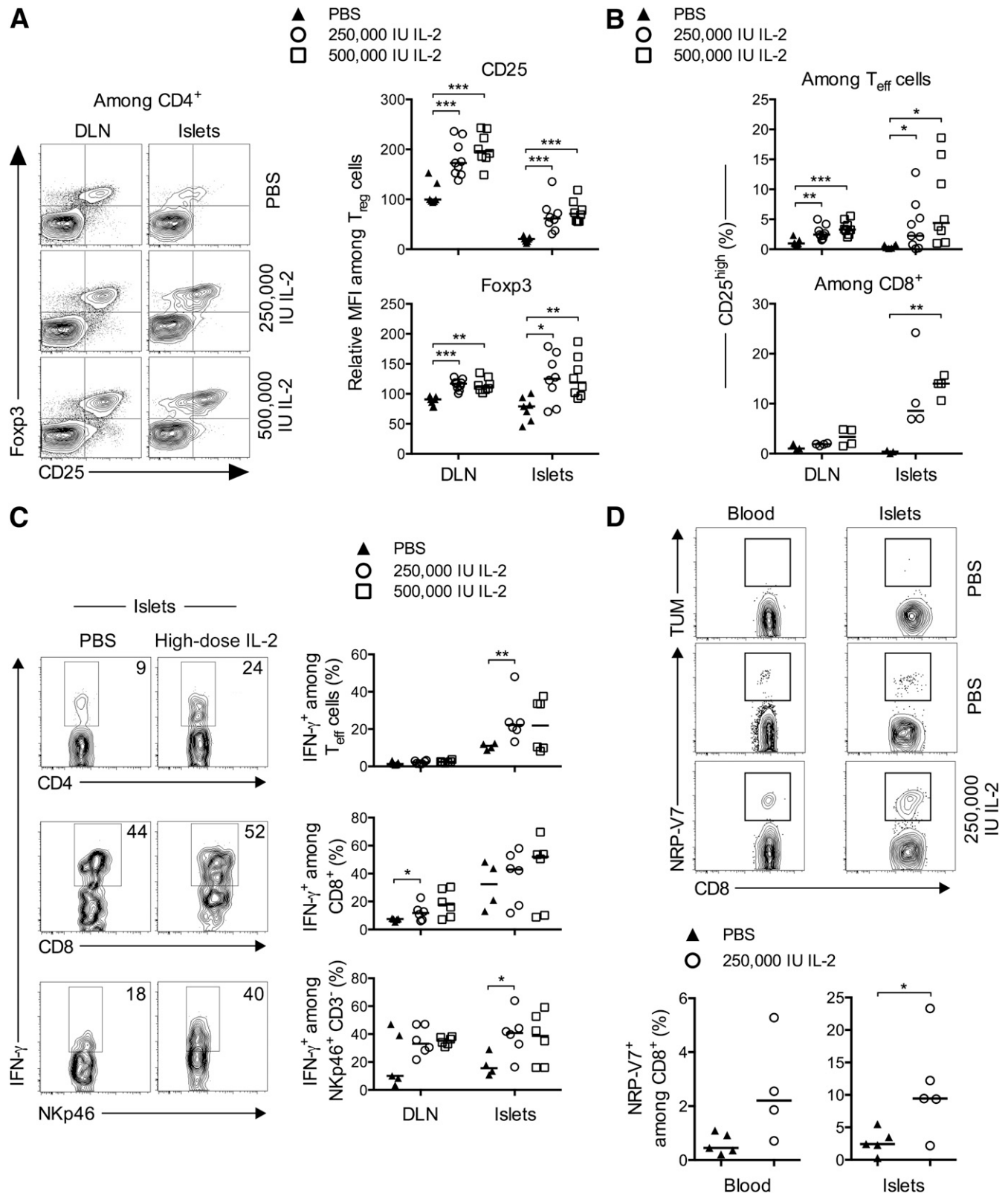

FIG. 4. Administration of high doses of IL-2 to NOD mice: effects on cell activation and cytokine production. Mice were treated as in Figure 2, and DLN and pancreas-infiltrating cells were analyzed by flow cytometry. *A*, *left*: Representative contour plots of Foxp3 and CD25 expression in CD4$^+$ T cells in indicated groups. *Right*: Relative mean fluorescence intensity (MFI) of Foxp3 and CD25 in T_{reg} cells expressed as the relative percentage of the MFI value in nondraining LNs of PBS-treated mice, which was assigned an arbitrary value of 100%. *B*: Percentages of CD25$^+$ cells among CD4$^+$ Foxp3$^-$ (T_{eff} cells) (*top*) and CD8$^+$ T cells (*bottom*). *C*: Representative contour plots of IFN-γ staining (*left*) and the percentage of IFN-γ–secreting cells (*right*) among islet-infiltrating CD4$^+$ Foxp3$^-$ (*top*), CD8$^+$ (*middle*), and NK cells (*bottom*) quantified after ex vivo stimulation with PMA-ionomycin. Data are cumulative of two to three independent experiments with four to nine mice per group. *$P < 0.05$; **$P < 0.01$; ***$P < 0.001$ (unpaired, two-tailed Student *t* test). *D*, *top*: Representative histograms of control TUM and NRP-V7 tretramer expression on CD8$^+$ T cells from blood and islets. *Bottom*: Percentage of NRP-V7$^+$ CD8$^+$ T cells among total CD8$^+$ T cells in blood (*left*) and in the pancreatic islets (*right*). Data are from one experiment, symbols represent individual mice, and horizontal lines represent the median. *$P < 0.05$ (unpaired, two-tailed Mann-Whitney test).

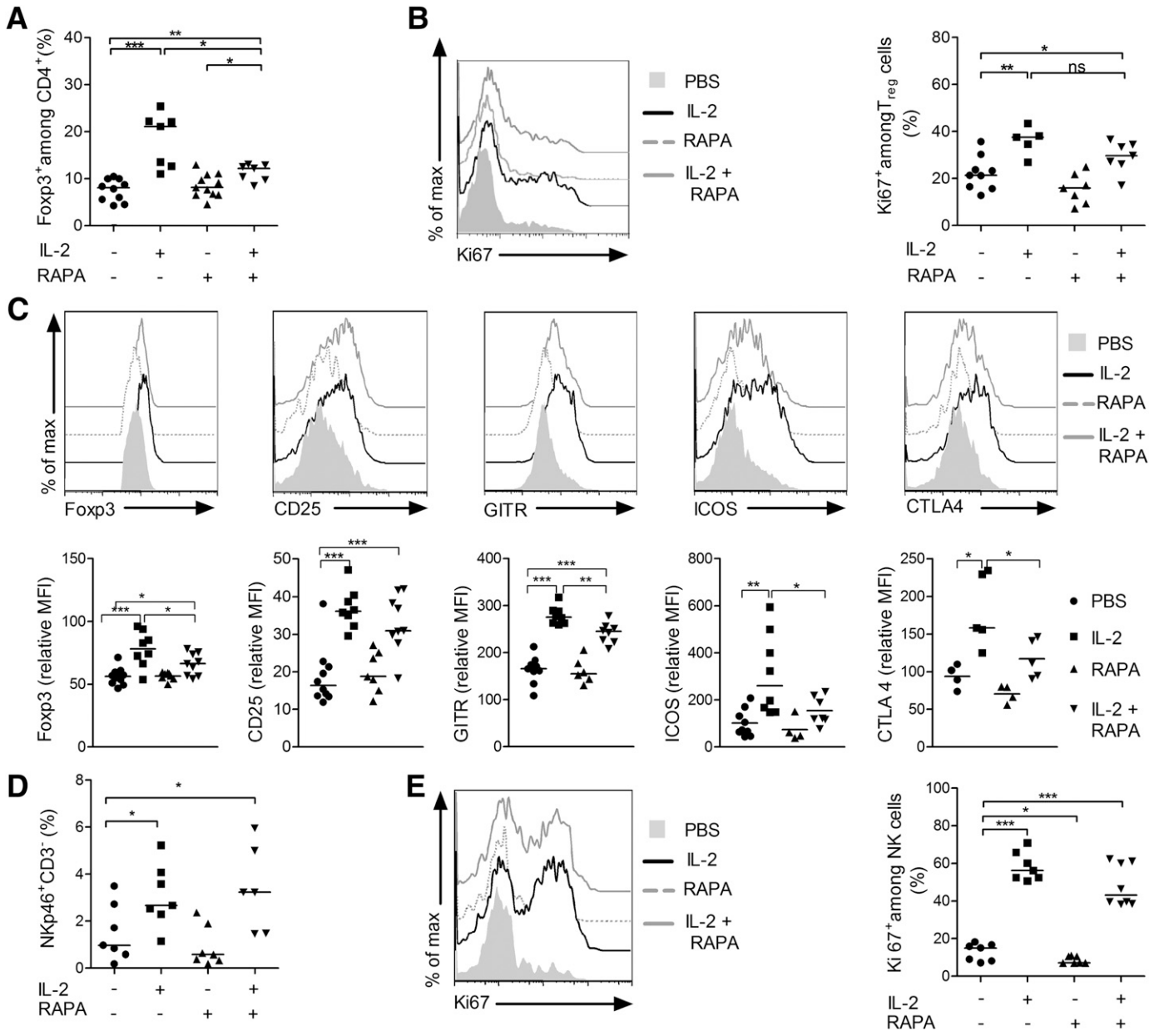

FIG. 5. Effects of combined low-dose IL-2 and RAPA on immune cells. Prediabetic female NOD mice 12–14 weeks of age were treated daily with PBS (n = 10), 25,000 IU IL-2 (n = 8), RAPA (1 mg/kg) (n = 12), or both (n = 10) over 5 days, and pancreas-infiltrating cells were collected and stained for flow cytometry analysis 2 h after the last treatment. *A*: Percentages of T_{reg} cells among $CD4^+$ T cells. *B*: Representative overlay histograms of Ki67 expression (*left*) and percentages of $Ki67^+$ T_{reg} cells (*right*) in indicated groups. *C*: Representative overlay histograms of Foxp3, CD25, GITR, ICOS, and CTLA-4 expression in T_{reg} cells (*top*) and the respective mean fluorescence intensity (MFI) (*bottom*) expressed as the relative percentage of the MFI value in nondraining LNs of untreated mice, which was assigned an arbitrary value of 100%. *D*: Percentages of $NKp46^+$ $CD3^-$ NK cells among pancreas-infiltrating cells. *E*: Representative overlay histograms of Ki67 expression (*left*) and percentages of $Ki67^+$ NK cells (*right*). Data are cumulative of four independent experiments, symbols represent individual mice, and horizontal lines represent the median. *$P < 0.05$; **$P < 0.01$; ***$P < 0.001$ (unpaired, two-tailed Student t test).

combined. Low-dose IL-2 treatment did not modify glucose homeostasis (Fig. 8*A* and *B*), in agreement with results obtained with high doses of IL-2 (Fig. 1*D*). However, RAPA/IL-2 combination induced elevated fasting blood glucose levels (Fig. 8*A*), and also RAPA- and RAPA/IL-2–treated mice displayed highly impaired glucose tolerance (Fig. 8*B*). Mechanistically, RAPA-induced glucose intolerance could be due to direct β-cell toxicity or to peripheral insulin resistance; we thus monitored β-cell division and performed insulin tolerance tests (Fig. 8*C* and *D*). Even if neither RAPA nor RAPA/IL-2 treatments visibly modified the response to an exogenous insulin boost, RAPA/IL-2 administration significantly reduced basal β-cell proliferation in vivo.

Finally, to better understand how RAPA alone or combined with IL-2 interfered with glucose homeostasis, we studied by microarray analysis the liver response to a glucose challenge. As depicted (Fig. 8*E* and Supplementary Fig. 1), the liver transcriptome signature was highly modified by IL-2 alone (81 genes) or combined with RAPA (40 genes), whereas fewer genes were affected by RAPA alone (16 genes). To retrieve relevant biological processes associated to the different treatments, we analyzed the canonical

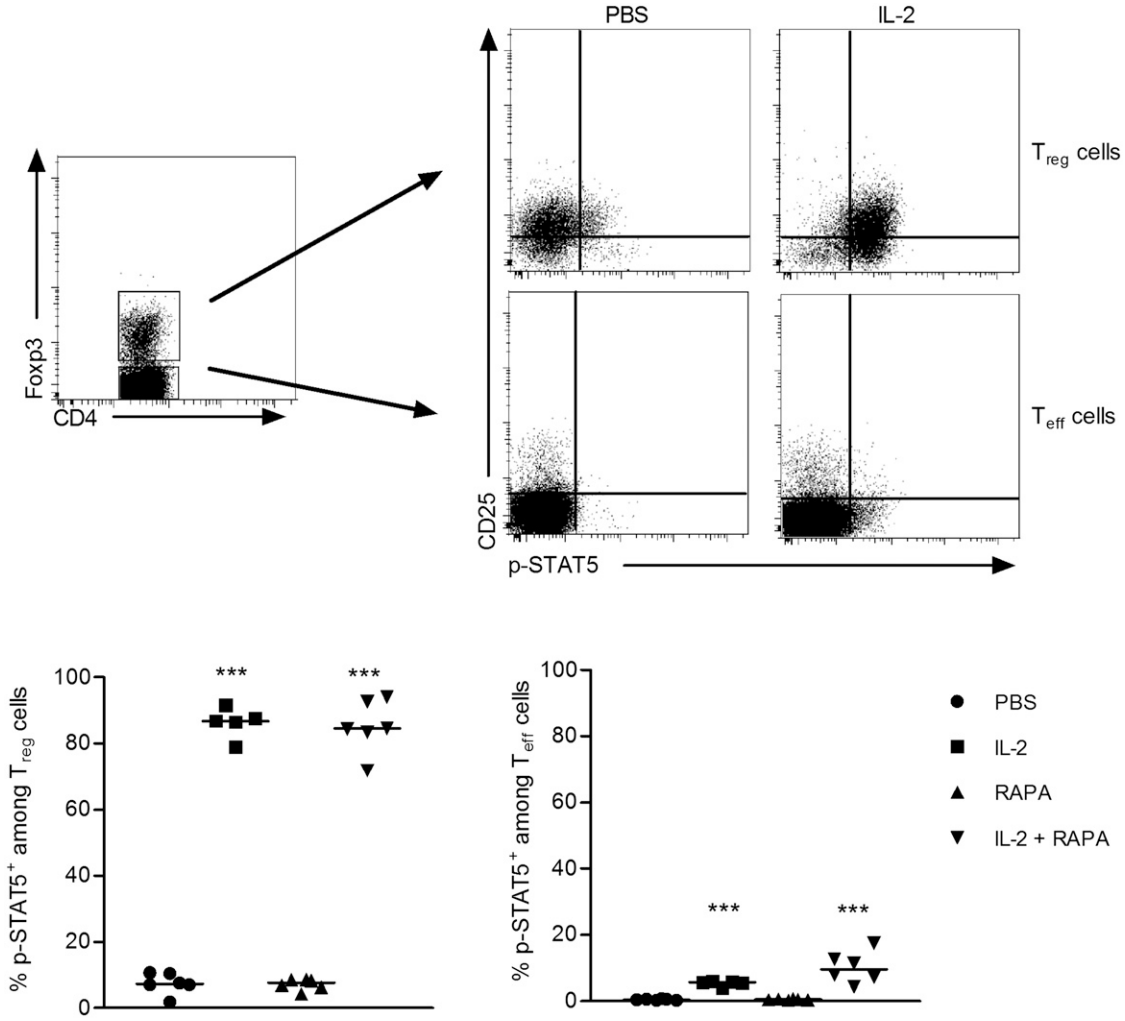

FIG. 6. IL-2 and RAPA effects on STAT5 phosphorylation. Prediabetic female NOD mice 12–16 weeks of age were injected with PBS, 1 mg/kg RAPA 16 and 2 h before analysis, 250,000 IU IL-2 2 h before the analysis, or the combined treatment (IL-2 + RAPA). Phosphorylation of STAT5 on T_{reg} cells ($CD4^+$ $Foxp3^+$ T cells) and T_{eff} cells ($CD4^+$ $Foxp3^-$ T cells) was determined by flow cytometry. Shown are the gating strategy to define the percentage of p-$STAT5^+$ T_{reg} and T_{eff} cells (*top*) and the percentage of p-$STAT5^+$ T_{reg} cells (*bottom left*) or T_{eff} cells (*bottom right*) in the DLN. Data are cumulative of three independent experiments, symbols represent individual mice, and horizontal lines represent the median. ***$P < 0.001$ (unpaired, two-tailed Student *t* test).

pathways that were most significant to our datasets (Supplementary Table 1). RAPA- and IL-2–modified transcripts were associated mainly with metabolic and immune pathways, respectively. Interestingly, RAPA/IL-2 combination modified other pathways than each drug alone, most of them involving metabolic functions. These data further document the complex effects of these drugs beyond immune modulation and may partially explain the associated detrimental effects on glucose homeostasis.

DISCUSSION

Low-dose IL-2 administration represents one promising approach (9) (clinical trial reg. no. NCT01353833, clinicaltrials.gov) among the novel immunotherapies being evaluated in T1D patients (4). We reasoned that we could enhance the efficiency with which IL-2 induces a tolerogenic state in NOD mice (9) by increasing its dose. However, higher IL-2 doses dramatically accelerated disease onset and demonstrated a toxicity that could even be lethal. Interestingly, female NOD mice were significantly more susceptible than males to diabetes induction, correlating with the higher incidence of spontaneous T1D in female mice (70%) compared with male mice (30%) (21). Additionally, high-dose IL-2–associated organ edema and insulitis appeared dissimilar in males and females, suggesting that IL-2–related side effects may be sex-dependent in the NOD mice.

T1D appeared in some of the mice treated with high-dose IL-2 despite substantial local and systemic increase in the frequency and activation of T_{reg} cells. Disease occurrence could be explained by the concurrent activation of T_{eff}, NK, B, and $CD8^+$ T cells, all of which have been implicated in T1D development (3,22). Of note, among $CD8^+$ T cells, islet-specific ones were enriched in the pancreas, potentially contributing to the destruction of the β-cells. Remarkably, high doses of IL-2 induced a previously unreported yet striking increase in $CD11b^+$ myeloid cells in the pancreas. Historically, macrophages have been regarded as mediators of insulitis (23). However, recently myeloid cells have been associated with T1D resistance and prevention in NOD mice (19,24,25). The role of different myeloid subpopulations in disease pathogenesis is nevertheless still largely unknown.

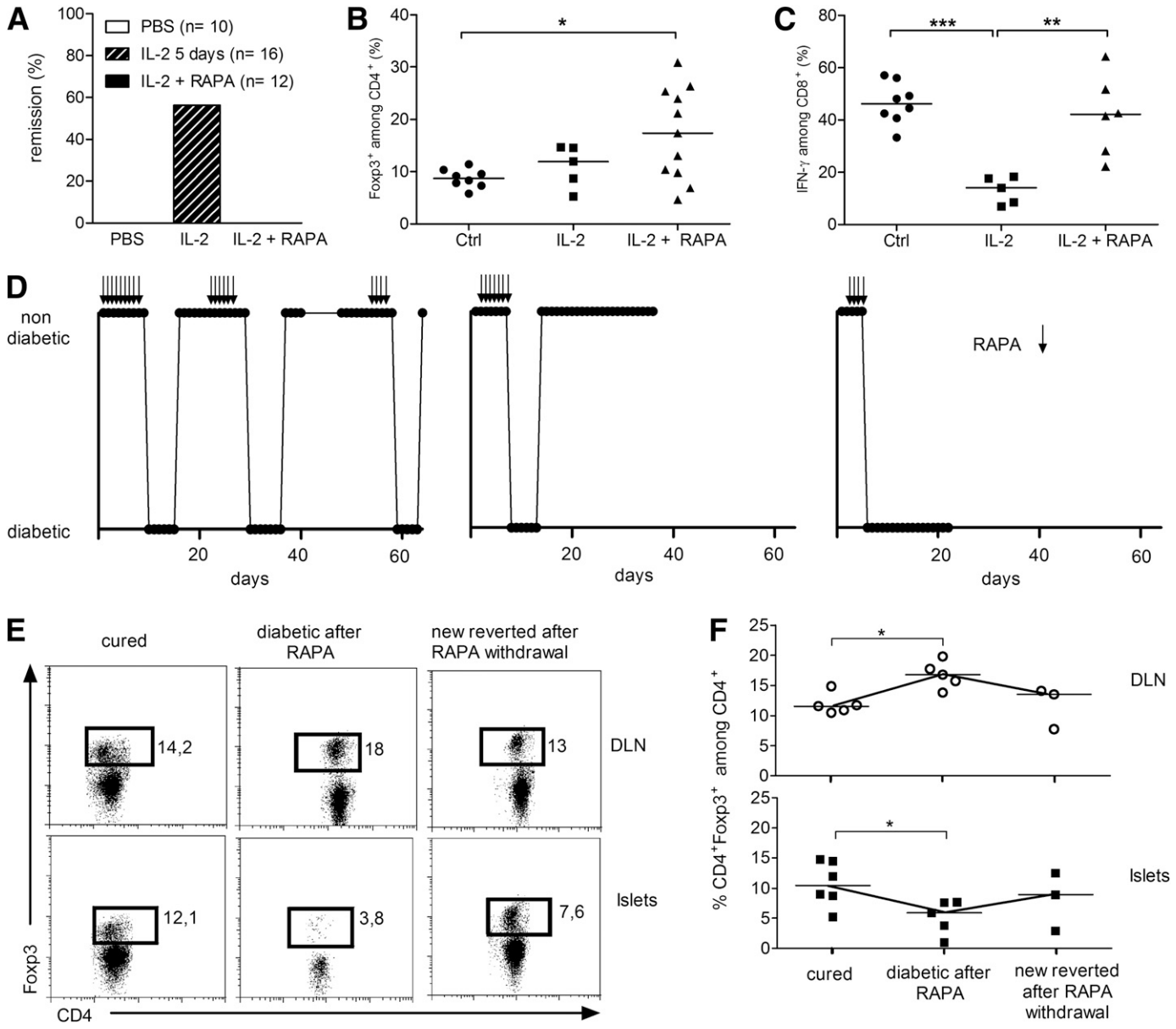

FIG. 7. RAPA abrogates IL-2–induced tolerance. New-onset diabetic NOD mice were treated daily for 5 days with PBS or 25,000 IU IL-2 or for 10 days with 1 mg/kg RAPA along with 25,000 IU IL-2. *A*: Percentage of T1D remission. *B* and *C*: Islet-infiltrating cells were analyzed 2 h after the last injection. *B*: Percentage of T_{reg} cells among CD4$^+$ T cells. *C*: Percentage of IFN-γ$^+$ cells among CD8$^+$ T cells quantified after ex vivo restimulation with PMA-ionomycin. Symbols represent individual mice, and horizontal bars are mean values. *$P < 0.05$; **$P < 0.01$; ***$P < 0.001$ (unpaired, two-tailed Student *t* test). *D*: New-onset diabetic NOD mice were cured by low-dose IL-2 and were treated with RAPA (1 mg/kg) 10 days after remission until the appearance of hyperglycemia (for 4 and up to 8 days). Arrows indicate RAPA administration. For some mice in which blood glucose levels normalized after RAPA withdrawal, a subsequent RAPA treatment was initiated after 10 days of normoglycemia, and, depending on the individual mice, this cycle could be repeated up to three times. Response to the treatment of three individual mice is shown. The term "diabetic" indicates blood glucose levels above 250 mg/dL or positive glycosuria, and "nondiabetic" indicates blood glucose levels below 250 mg/dL or negative glycosuria. *E* and *F*: The percentage of CD4$^+$ Foxp3$^+$ T cells among CD4$^+$ cells was analyzed by flow cytometry in the DLN and the islets of individual mice at different points during treatment. *E*: Representative dot plots of Foxp3 and CD4 staining among CD4$^+$ T cells. *F*: Percentage of T_{reg} cells among CD4$^+$ T cells in the DLN (*top*) and in the islets (*bottom*). Symbols represent individual mice, and horizontal lines represent the median. Cured, IL-2 cured mice ($n = 6$); diabetic after RAPA, mice that became diabetic under RAPA treatment ($n = 5$); new reverted after RAPA withdrawal, mice that regained normal glucose homeostasis after RAPA withdrawal ($n = 3$). *$P < 0.05$ (unpaired, two-tailed Mann-Whitney test).

Overall, higher doses of IL-2 resulted in a shift from immune tolerance to overt destructive autoimmunity. In the context of human therapy, these results highlight the need to perform thorough immunomonitoring of the broad effects of IL-2 so as to determine the dose that would uniquely act on T_{reg} cells or other regulatory populations.

The potent immunosuppressive properties of RAPA are associated with its capacity to block cell cycle progression and induce T-cell anergy and depletion (26), thus impacting on T-cell differentiation and function. In our model, RAPA specifically dampened the IL-2 effect on pancreatic T_{reg} cells. Notably, diabetic animals receiving IL-2/RAPA combination showed higher frequencies of pancreatic T_{reg} cells compared with treatment with IL-2 alone, which nevertheless were associated with inefficient control of IFN-γ production by infiltrating T cells. These T_{reg} cells could originate from the expansion of preexisting natural T_{reg} cells or from the generation of induced T_{reg} cells from T_{eff}

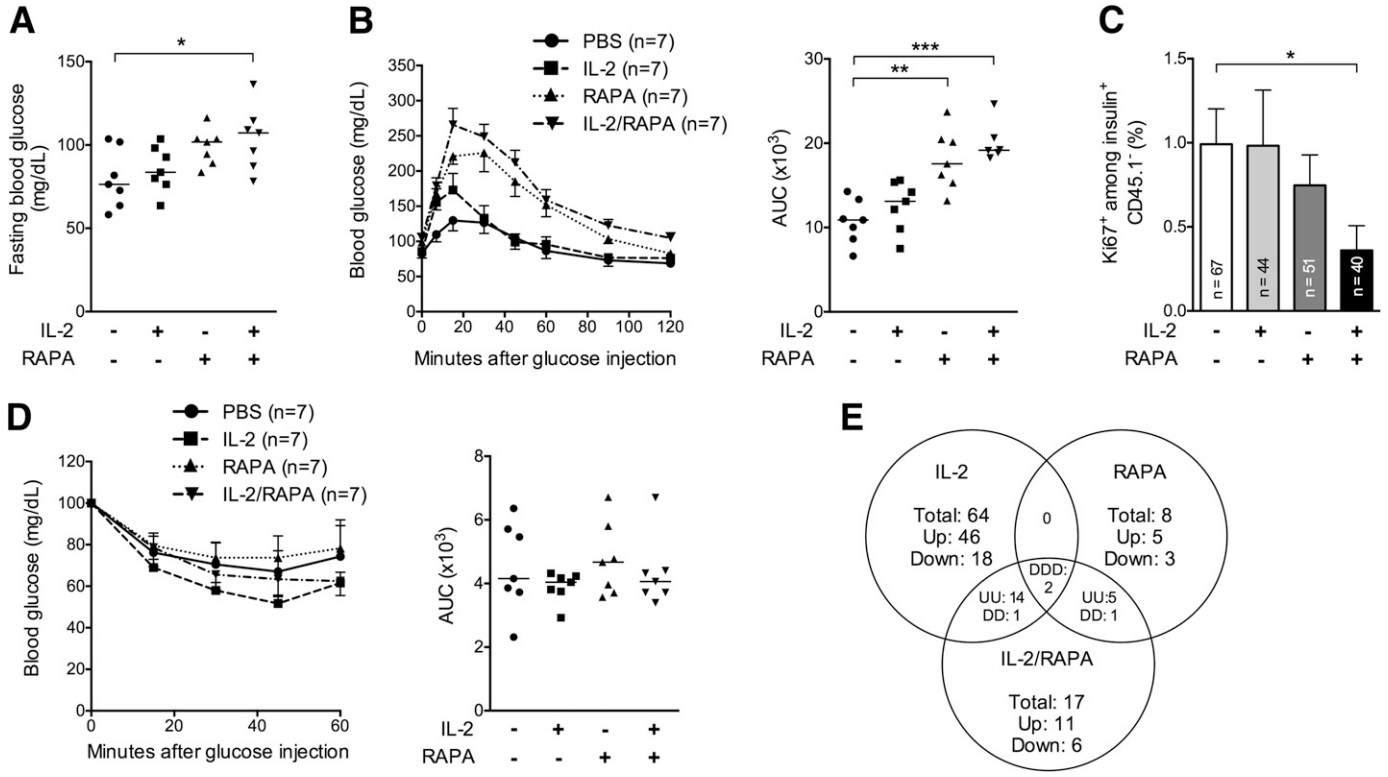

FIG. 8. A short course of RAPA alone or combined with IL-2 induces glucose intolerance. Prediabetic female NOD mice were treated for 5 days with PBS, 25,000 IU IL-2, 1 mg/kg RAPA, or IL-2 and RAPA combined. *A*, *B*, and *E*: On day 5, an IPGTT was performed after an overnight fast or mice were killed 4 h after the glucose bolus for transcriptome analysis of the liver. *A*: Fasting blood glucose levels were determined before glucose injection. *B*: Blood glucose levels and area under the blood glucose curve (AUC) of the treated mice of the different groups (n = 7–8 per group). Data are cumulative of two independent experiments with seven mice per group. Symbols represent individual mice, and horizontal lines represent the median. *P < 0.05; **P < 0.01; ***P < 0.001 (unpaired, two-tailed Student t test). *C*: Percentage of Ki67$^+$ cells among total β-cells (insulin$^+$ CD45.1$^-$) analyzed at day 5. Each column represents the mean ± SEM of all islets counted for all mice of the same group (n = 3–4 per group). *P < 0.05 (Mann-Whitney test). *D*: On day 5, an ITT was performed after a 4 h fast. Shown are blood glucose levels and area under the blood glucose curve of the treated mice of the different groups (n = 7 per group). Symbols represent individual mice, and horizontal lines represent the median. *E*: Venn diagram comparing differentially expressed genes in the liver after glucose challenge of mice in IL-2 vs. PBS, IL-2/RAPA vs. PBS, and RAPA vs. PBS groups. The threshold for differential expression was defined as 1.5-fold changes in expression with overlapping probes discarded. Each number represents the number of genes in each subgroup: total number of genes (Total), and upregulated (Up, or U) and downregulated (Down, or D) probes from reference PBS. Each dataset was derived from three biologically independent replicate samples.

cells, probably favored by the proinflammatory environment in the islets (27).

We could not attribute the deleterious impact of IL-2/RAPA combination on T_{reg}-cell function to interference of RAPA on IL-2–mediated activation of STAT-5. However, although T_{reg} cells are less dependent for survival on the AKT/mammalian target of RAPA pathway than are T_{eff} cells (28), it is possible that RAPA inhibition of this pathway may still affect IL-2 action on T_{reg} cells (29,30).

NK cells have been described as having no role (31) or a pathogenic role in NOD T1D (32). In humans, they have been seen as either potentially harmful (33,34) or regulatory (35,36). Thus, their role in T1D progression is still debated. Human NK cells have been found to be significantly increased upon IL-2 administration (37,38), notably in T1D patients (30). In our model, after IL-2 administration NK cells rapidly expanded in the pancreas after IL-2 administration. Of note, the effect of IL-2 on NK cells was not affected by the addition of RAPA, raising the hypothesis that, in comparison with IL-2 monotherapy, RAPA/IL-2 combination may negatively impact on pancreatic T_{reg} cells while failing to control IL-2–boosted NK cells. This is reminiscent of the previous observation that punctual ablation of T_{reg} cells in NOD-BDC2.5 TCR transgenic mice resulted in a fulminant form of diabetes characterized by an initial burst in NK cell function, which led to IFN-γ−dependent activation of pathogenic T-cell populations (39).

Although our data suggest that the deleterious effects of RAPA in IL-2–treated NOD mice may be related to its action on T_{reg}-cell function or trafficking, we also found that a short course of RAPA and IL-2 at low doses significantly impaired glucose homeostasis. There have been some reports of renal transplant patients who received long-term treatment with RAPA becoming at risk for developing new-onset diabetes, associated with abnormal glucose and lipid homeostasis and with reduced insulin sensitivity (40). Furthermore, in rodents, long-term RAPA treatment severely impairs glucose tolerance, affecting hepatic gluconeogenesis (41,42), adipocyte lipid uptake (41), skeletal muscle insulin sensitivity (43), and β-cell homeostasis (41). However, RAPA alone prevents T1D development in NOD mice (13,44) and has been reported to improve T_{reg}-cell suppressive function in T1D patients (12). Here, we demonstrate that RAPA administration even for a short period and at doses two to five times lower than those reported in the literature (41,42); impaired glucose tolerance, as previously suggested (14); and modified liver glucose metabolism in the NOD model. Moreover, when combined with IL-2, the negative effects on glucose metabolism were broadened, also inducing elevated basal blood glucose levels and

impairing β-cell proliferation. Interestingly, our results showing that RAPA restored diabetes in NOD mice, which had been previously cured of new-onset disease by IL-2 treatment, evoke RAPA effects counteracting anti-CD3 treatment in NOD mice (14).

Recently, a clinical trial testing RAPA/IL-2 combined therapy in new onset T1D patients was halted due to a transient drop in C-peptide levels in all patients, despite effective T_{reg}-cell induction (30). Our results showing that RAPA breaks IL-2–induced tolerance and that, in combination with IL-2, it induces glucose intolerance, help to explain the inefficacy and deleterious consequences of the combined treatment in T1D. However, the RAPA/IL-2 combination can be efficient at boosting T_{reg} cells and inducing tolerance in graft-versus-host disease (37,45). The latter results, which were observed in hosts devoid of the metabolic alterations associated with T1D, demonstrate the different potential outcomes of the combined treatment depending on the underlying pathology. And even when referring to T1D, it is surprising to observe that the RAPA and IL-2 combination can have a completely different outcome in preventive or curative schedules in the NOD mice (13). Probably, in prediabetic mice, the effects of RAPA are not strong enough to cause hyperglycemia because, at odds with already diabetic mice, there are enough healthy islets to compensate for the negative effects of RAPA, at least for a short-term treatment.

Our results, together with the accumulated experience in the use of IL-2 and RAPA in the context of T1D prevention or reversal (see recapitulation in Supplementary Table 2), help define the limitations of the application of these drugs in T1D and may contribute to the design of improved IL-2–based therapy.

ACKNOWLEDGMENTS

E.P. has received Agence Nationale de la Recherche grant ANR-09-GENO-006-01 and an INSERM/Direction Générale de l'Offre de Soins 2011 grant. O.B. has received a University of Zurich Fonds zur Förderung des Akademischen Nachwuchses grant. A.B. and L.P. were supported by the Ministère de la Recherche.

E.P. has received a European Foundation for the Study of Diabetes/Juvenile Diabetes Research Foundation International/Novo Nordisk 2011 grant. E.P. is the inventor of a patent application related to the use of low-dose IL-2 owned by her public institutions. No other potential conflicts of interest relevant to this article were reported.

A.B., L.P., G.F., J.W., O.B., and E.P. designed and performed the experiments and analyzed data. N.C and W.C. performed and analyzed microarray experiments. E.P. conceived the project. A.B., L.P., and E.P. wrote the manuscript. A.H. and all the authors discussed the results and commented on the manuscript. E.P. is the guarantor of this work and, as such, had full access to all the data in the study and takes responsibility for the integrity of the data and the accuracy of the data analysis.

The authors thank Pere Santamaria, University of Calgary, Canada, for kindly providing the NRP-V7 and TUM tetramers, and Benoit Salomon, INSERM U959, Paris; Olivier Boyer, INSERM U905, Rouen; and José Cohen, INSERM U855, Créteil, for constructive and critical reading of the manuscript. The authors especially thank Bertrand Blondeau, UMRS 872, Paris, for his valuable advice and technical help and Pedro Carranza (supported by Cardiovascular Diseases, Diabetes and Obesity) Ile-de-France, INSERM U959, Paris, and Hanem Sadek, INSERM U959, Paris, for technical help. The authors thank Christelle Enond, Flora Issert, François Bodin, and Serban Morosan (all from the Centre d'Exploration Fonctionnelle, Université Pierre et Marie Curie) for taking good care of the mice.

REFERENCES

1. Bach JF. Insulin-dependent diabetes mellitus as an autoimmune disease. Endocr Rev 1994;15:516–542
2. Sreenan S, Pick AJ, Levisetti M, Baldwin AC, Pugh W, Polonsky KS. Increased beta-cell proliferation and reduced mass before diabetes onset in the nonobese diabetic mouse. Diabetes 1999;48:989–996
3. Bluestone JA, Herold K, Eisenbarth G. Genetics, pathogenesis and clinical interventions in type 1 diabetes. Nature 2010;464:1293–1300
4. Waldron-Lynch F, Herold KC. Immunomodulatory therapy to preserve pancreatic β-cell function in type 1 diabetes. Nat Rev Drug Discov 2011;10:439–452
5. Atkinson MA, Leiter EH. The NOD mouse model of type 1 diabetes: as good as it gets? Nat Med 1999;5:601–604
6. Chatenoud L, Thervet E, Primo J, Bach JF. Anti-CD3 antibody induces long-term remission of overt autoimmunity in nonobese diabetic mice. Proc Natl Acad Sci USA 1994;91:123–127
7. Bach JF. Anti-CD3 antibodies for type 1 diabetes: beyond expectations. Lancet 2011;378:459–460
8. Tang Q, Adams JY, Penaranda C, et al. Central role of defective interleukin-2 production in the triggering of islet autoimmune destruction. Immunity 2008;28:687–697
9. Grinberg-Bleyer Y, Baeyens A, You S, et al. IL-2 reverses established type 1 diabetes in NOD mice by a local effect on pancreatic regulatory T cells. J Exp Med 2010;207:1871–1878
10. Abraham RT, Wiederrecht GJ. Immunopharmacology of rapamycin. Annu Rev Immunol 1996;14:483–510
11. Piemonti L, Maffi P, Monti L, et al. Beta cell function during rapamycin monotherapy in long-term type 1 diabetes. Diabetologia 2011;54:433–439
12. Monti P, Scirpoli M, Maffi P, et al. Rapamycin monotherapy in patients with type 1 diabetes modifies CD4+CD25+FOXP3+ regulatory T-cells. Diabetes 2008;57:2341–2347
13. Rabinovitch A, Suarez-Pinzon WL, Shapiro AM, Rajotte RV, Power R. Combination therapy with sirolimus and interleukin-2 prevents spontaneous and recurrent autoimmune diabetes in NOD mice. Diabetes 2002;51:638–645
14. Valle A, Jofra T, Stabilini A, Atkinson M, Roncarolo MG, Battaglia M. Rapamycin prevents and breaks the anti-CD3-induced tolerance in NOD mice. Diabetes 2009;58:875–881
15. Cassan C, Piaggio E, Zappulla JP, et al. Pertussis toxin reduces the number of splenic Foxp3+ regulatory T cells. J Immunol 2006;177:1552–1560
16. Grinberg-Bleyer Y, Saadoun D, Baeyens A, et al. Pathogenic T cells have a paradoxical protective effect in murine autoimmune diabetes by boosting Tregs. J Clin Invest 2010;120:4558–4568
17. Krieg C, Létourneau S, Pantaleo G, Boyman O. Improved IL-2 immunotherapy by selective stimulation of IL-2 receptors on lymphocytes and endothelial cells. Proc Natl Acad Sci USA 2010;107:11906–11911
18. Fu W, Wojtkiewicz G, Weissleder R, Benoist C, Mathis D. Early window of diabetes determinism in NOD mice, dependent on the complement receptor CRIg, identified by noninvasive imaging. Nat Immunol 2012;13:361–368
19. Trudeau JD, Kelly-Smith C, Verchere CB, et al. Prediction of spontaneous autoimmune diabetes in NOD mice by quantification of autoreactive T cells in peripheral blood. J Clin Invest 2003;111:217–223
20. Battaglia M, Stabilini A, Roncarolo MG. Rapamycin selectively expands CD4+CD25+FoxP3+ regulatory T cells. Blood 2005;105:4743–4748
21. Billiard F, Litvinova E, Saadoun D, et al. Regulatory and effector T cell activation levels are prime determinants of in vivo immune regulation. J Immunol 2006;177:2167–2174
22. van Belle TL, Coppieters KT, von Herrath MG. Type 1 diabetes: etiology, immunology, and therapeutic strategies. Physiol Rev 2011;91:79–118
23. Jansen A, Homo-Delarche F, Hooijkaas H, Leenen PJ, Dardenne M, Drexhage HA. Immunohistochemical characterization of monocytes-macrophages and dendritic cells involved in the initiation of the insulitis and beta-cell destruction in NOD mice. Diabetes 1994;43:667–675
24. Hu C, Du W, Zhang X, Wong FS, Wen L. The role of Gr1+ cells after anti-CD20 treatment in type 1 diabetes in nonobese diabetic mice. J Immunol 2012;188:294–301
25. Yin B, Ma G, Yen CY, et al. Myeloid-derived suppressor cells prevent type 1 diabetes in murine models. J Immunol 2010;185:5828–5834
26. Thomson AW, Turnquist HR, Raimondi G. Immunoregulatory functions of mTOR inhibition. Nat Rev Immunol 2009;9:324–337

27. Battaglia M, Stabilini A, Draghici E, et al. Induction of tolerance in type 1 diabetes via both CD4+CD25+ T regulatory cells and T regulatory type 1 cells. Diabetes 2006;55:1571–1580
28. Delgoffe GM, Kole TP, Zheng Y, et al. The mTOR kinase differentially regulates effector and regulatory T cell lineage commitment. Immunity 2009;30: 832–844
29. Kuo CJ, Chung J, Fiorentino DF, Flanagan WM, Blenis J, Crabtree GR. Rapamycin selectively inhibits interleukin-2 activation of p70 S6 kinase. Nature 1992;358:70–73
30. Long SA, Rieck M, Sanda S, et al.; Diabetes TrialNet and the Immune Tolerance Network. Rapamycin/IL-2 combination therapy in patients with type 1 diabetes augments Tregs yet transiently impairs β-cell function. Diabetes 2012;61:2340–2348
31. Beilke JN, Meagher CT, Hosiawa K, Champsaur M, Bluestone JA, Lanier LL. NK cells are not required for spontaneous autoimmune diabetes in NOD mice. PLoS One 2012;7:e36011
32. Gur C, Porgador A, Elboim M, et al. The activating receptor NKp46 is essential for the development of type 1 diabetes. Nat Immunol 2010;11: 121–128
33. Gur C, Enk J, Kassem SA, et al. Recognition and killing of human and murine pancreatic beta cells by the NK receptor NKp46. J Immunol 2011; 187:3096–3103
34. Schleinitz N, Vély F, Harlé JR, Vivier E. Natural killer cells in human autoimmune diseases. Immunology 2010;131:451–458
35. Li Z, Lim WK, Mahesh SP, Liu B, Nussenblatt RB. Cutting edge: in vivo blockade of human IL-2 receptor induces expansion of CD56(bright) regulatory NK cells in patients with active uveitis. J Immunol 2005;174:5187–5191
36. Bielekova B, Catalfamo M, Reichert-Scrivner S, et al. Regulatory CD56 (bright) natural killer cells mediate immunomodulatory effects of IL-2Ralpha-targeted therapy (daclizumab) in multiple sclerosis. Proc Natl Acad Sci USA 2006;103:5941–5946
37. Koreth J, Matsuoka K, Kim HT, et al. Interleukin-2 and regulatory T cells in graft-versus-host disease. N Engl J Med 2011;365:2055–2066
38. Saadoun D, Rosenzwajg M, Joly F, et al. Regulatory T-cell responses to low-dose interleukin-2 in HCV-induced vasculitis. N Engl J Med 2011;365: 2067–2077
39. Feuerer M, Shen Y, Littman DR, Benoist C, Mathis D. How punctual ablation of regulatory T cells unleashes an autoimmune lesion within the pancreatic islets. Immunity 2009;31:654–664
40. Johnston O, Rose CL, Webster AC, Gill JS. Sirolimus is associated with new-onset diabetes in kidney transplant recipients. J Am Soc Nephrol 2008;19:1411–1418
41. Houde VP, Brûlé S, Festuccia WT, et al. Chronic rapamycin treatment causes glucose intolerance and hyperlipidemia by upregulating hepatic gluconeogenesis and impairing lipid deposition in adipose tissue. Diabetes 2010;59:1338–1348
42. Lamming DW, Ye L, Katajisto P, et al. Rapamycin-induced insulin resistance is mediated by mTORC2 loss and uncoupled from longevity. Science 2012;335:1638–1643
43. Cunningham JT, Rodgers JT, Arlow DH, Vazquez F, Mootha VK, Puigserver P. mTOR controls mitochondrial oxidative function through a YY1-PGC-1alpha transcriptional complex. Nature 2007;450:736–740
44. Baeder WL, Sredy J, Sehgal SN, Chang JY, Adams LM. Rapamycin prevents the onset of insulin-dependent diabetes mellitus (IDDM) in NOD mice. Clin Exp Immunol 1992;89:174–178
45. Shin HJ, Baker J, Leveson-Gower DB, Smith AT, Sega EI, Negrin RS. Rapamycin and IL-2 reduce lethal acute graft-versus-host disease associated with increased expansion of donor type CD4+CD25+Foxp3+ regulatory T cells. Blood 2011;118:2342–2350